AMERICAN SOCIETY FOR MICROBIOLOGY | Molecular and Cellular Biology®

RESEARCH ARTICLE

Replication Protein A Phosphorylation Facilitates RAD52-Dependent Homologous Recombination in BRCA-Deficient Cells

Alison C. Carley,[a,b] Manisha Jalan,[c] Shyamal Subramanyam,[c] Rohini Roy,[c] Gloria E. O. Borgstahl,[d,e] Simon N. Powell[a,c]

[a]Molecular Biology Program, Memorial Sloan Kettering Cancer Center, New York, New York, USA
[b]Molecular Biology Department, Weill Cornell Graduate School of Medical Sciences, New York, New York, USA
[c]Department of Radiation Oncology, Memorial Sloan Kettering Cancer Center, New York, New York, USA
[d]Eppley Institute for Research in Cancer and Allied Diseases, University of Nebraska Medical Center, Omaha, Nebraska, USA
[e]Fred & Pamela Buffett Cancer Center, University of Nebraska Medical Center, Omaha, Nebraska, USA

Alison C. Carley and Manisha Jalan contributed equally to this work. Author order was determined both alphabetically and in order of increasing seniority.

ABSTRACT Loss of RAD52 is synthetically lethal in BRCA-deficient cells, owing to its role in backup homologous recombination (HR) repair of DNA double-strand breaks (DSBs). In HR in mammalian cells, DSBs are processed to single-stranded DNA (ssDNA) overhangs, which are then bound by replication protein A (RPA). RPA is exchanged for RAD51 by mediator proteins: in mammals, BRCA2 is the primary mediator; however, RAD52 provides an alternative mediator pathway in BRCA-deficient cells. RAD51 stimulates strand exchange between homologous DNA duplexes, a critical step in HR. RPA phosphorylation and dephosphorylation are important for HR, but its effect on RAD52 mediator function is unknown. Here, we show that RPA phosphorylation is required for RAD52 to salvage HR in BRCA-deficient cells. In BRCA2-depleted human cells, in which the only available mediator pathway is RAD52 dependent, the expression of a phosphorylation-deficient RPA mutant reduced HR. Furthermore, RPA-phosphomutant cells showed reduced association of RAD52 with RAD51. Interestingly, there was no effect of RPA phosphorylation on RAD52 recruitment to repair foci. Finally, we show that RPA phosphorylation does not affect RAD52-dependent ssDNA annealing. Thus, although RAD52 can be recruited independently of RPA's phosphorylation status, RPA phosphorylation is required for RAD52's association with RAD51 and its subsequent promotion of RAD52-mediated HR.

KEYWORDS BRCA deficient, DNA repair, RAD52, RPA phosphorylation, double-strand-break repair, homologous recombination

DNA double-strand breaks (DSBs) are the most deleterious type of DNA damage and arise during endogenous processes, such as DNA replication, or after exposure to DNA-damaging agents, such as ionizing radiation or topoisomerase poisons (1). DSBs are resolved predominately by two main pathways: homologous recombination (HR) and nonhomologous end joining (NHEJ). HR accurately repairs DSBs, thereby contributing significantly to the maintenance of genome integrity. In HR, DSBs are resected to generate single-stranded DNA (ssDNA) overhangs, which are bound by the heterotrimeric ssDNA binding complex, replication protein A (RPA) (1–5). RPA is exchanged for the RAD51 recombinase protein, which then performs homology search and strand invasion. In mammalian cells, BRCA2 mediates this RAD51 filament formation on RPA-coated ssDNA and stimulates RAD51 strand invasion (6, 7). Notably, *Saccharomyces cerevisiae* lacks BRCA2—instead, RAD52 mediates this function in yeast (8, 9). As BRCA2 serves as the primary recombination mediator, the role of RAD52 in mammalian cells is poorly understood. While *Rad52*-deficient mice show no survival deficiencies or sensitivity to ionizing radiation, inactivation of the protein leads to slightly reduced HR, as measured by gene targeting (10). RAD52 is also inefficient at displacing RPA

Address correspondence to Simon N. Powell, powells@mskcc.org.

The authors declare no conflict of interest.

Received 9 December 2021
Returned for modification 14 December 2021
Accepted 15 December 2021
Accepted manuscript posted online 20 December 2021
Published 17 February 2022

and stimulating strand exchange *in vitro*, and RAD52 is not essential for RAD51 function or HR (6, 10, 11). Prior evidence suggests that in BRCA-deficient cells the RAD52 protein is integral to the mediator activity in HR (12, 13), which depends on the annealing activity of RAD52 on resected DNA (14), on interaction with RAD51 (15), and on interaction with other proteins that are part of the HR pathway (16). In BRCA2-deficient human cancer cell lines, the depletion of RAD52 reduces cell survival and proliferation, suggesting a synthetically lethal relationship between the two proteins (13). Further, RAD52 is necessary for RAD51-mediated HR in BRCA2-deficient cells (13). RAD52 mediator function is independent of BRCA2, since its recruitment to damaged DNA is not affected by the presence of the BRCA2 protein, and it interacts with RAD51 independently of BRCA2 (13). These observations suggest a critical role for a RAD52-mediated backup pathway for HR in mammalian cells. That is, in the presence of BRCA2, RAD52 has little effect on HR and viability, whereas in BRCA2-deficient cells, RAD52 is essential for viability and for the repair of DSBs via HR (13). The additional factors required for this backup pathway are unknown and of significant interest in RAD52 research.

RPA is a critical part of the DNA repair machinery and key to the maintenance of genome integrity (17). Binding of RPA to resected ssDNA helps recruit several checkpoint proteins which initiate the DNA damage response (18). Loss of RPA arrests growth in *Saccharomyces cerevisiae* (19) and is embryonically lethal in mice. Haploinsufficiency of RPA in mammals is known to be tumorigenic (20, 21). In mammalian cells, RAD52 has been shown to interact with the RPA2 subunit of the RPA complex, and facilitates HR in mammalian cells (22). RPA2 is hyperphosphorylated in response to DNA damage by the activity of phosphoinositide 3-kinase (PI3K)-related protein kinases (PIKK): ATM, ATR and DNA-PK (23–26). The interplay between these three kinases is an intricate and tightly regulated process that is dependent upon the kind of insult experienced by the cell. This posttranslational modification is necessary for the recruitment of RAD51 recombinase to DNA break sites and is critical for HR (27, 28). Furthermore, dephosphorylation of RPA2 by PP4 and PP2A phosphatases is also essential for optimal HR (29, 30). Although posttranslational regulation of RPA has been extensively studied (26), the mechanisms underlying how RPA phosphorylation status affects RAD52 function is poorly understood. *In vitro* studies have demonstrated that that RAD52 associates in a RPA-RAD52-ssDNA complex when RPA is phosphorylated (pRPA), which facilitates enhanced RAD52 interactions with ssDNA (31). However, these observations are yet to be confirmed in mammalian cells.

Here, by using phosphorylation-deficient mutants in mammalian cell lines as well as biochemical characterization of regulation of RAD52 by RPA, we address how RPA phosphorylation affects RAD52 function. Our studies determined that RPA phosphorylation affects RAD52-mediated HR directly. Using endonuclease-induced DSBs, we show that RPA phosphorylation-deficient mutants have reduced RAD52-dependent HR and RAD51 recruitment to DSBs. We also show that the interaction of RPA and RAD52 is not significantly affected by RPA hyperphosphorylation. Furthermore, in biochemical studies, we observe that phosphorylation of RPA does not alter the annealing of ssDNA by RAD52, an important characteristic of RAD52 function. How RAD52 functions as a RAD51 mediator in HR was the focus of this investigation. A better understanding of the regulation of RAD52 function in HR and DNA repair is paramount to the development of therapeutic strategies that exploit tumor-specific synthetic lethality of RAD52.

RESULTS

RAD52-mediated HR is promoted by RPA hyperphosphorylation. Hyperphosphorylation of RPA is required for the recruitment of RAD51 and other proteins critical to HR in mammalian cells (27, 28). However, the effects of RPA phosphorylation on RAD52 function are poorly understood. In order to study the effect of RPA hyperphosphorylation on RAD52-mediated HR, we used the DR-GFP assay (32). This assay tracks the restoration of green fluorescent protein (GFP) expression resulting from a gene conversion event induced by an I-SceI DSB. When an I-SceI break in a fluorescence defective *SceGFP* construct is repaired by HR with the *iGFP* gene fragment serving as a repair template, a functional *GFP* gene results and is expressed (32). The percentage of cells expressing GFP can then be determined using flow cytometry analysis. Using a system similar to that used in other studies of RPA phosphorylation (33),

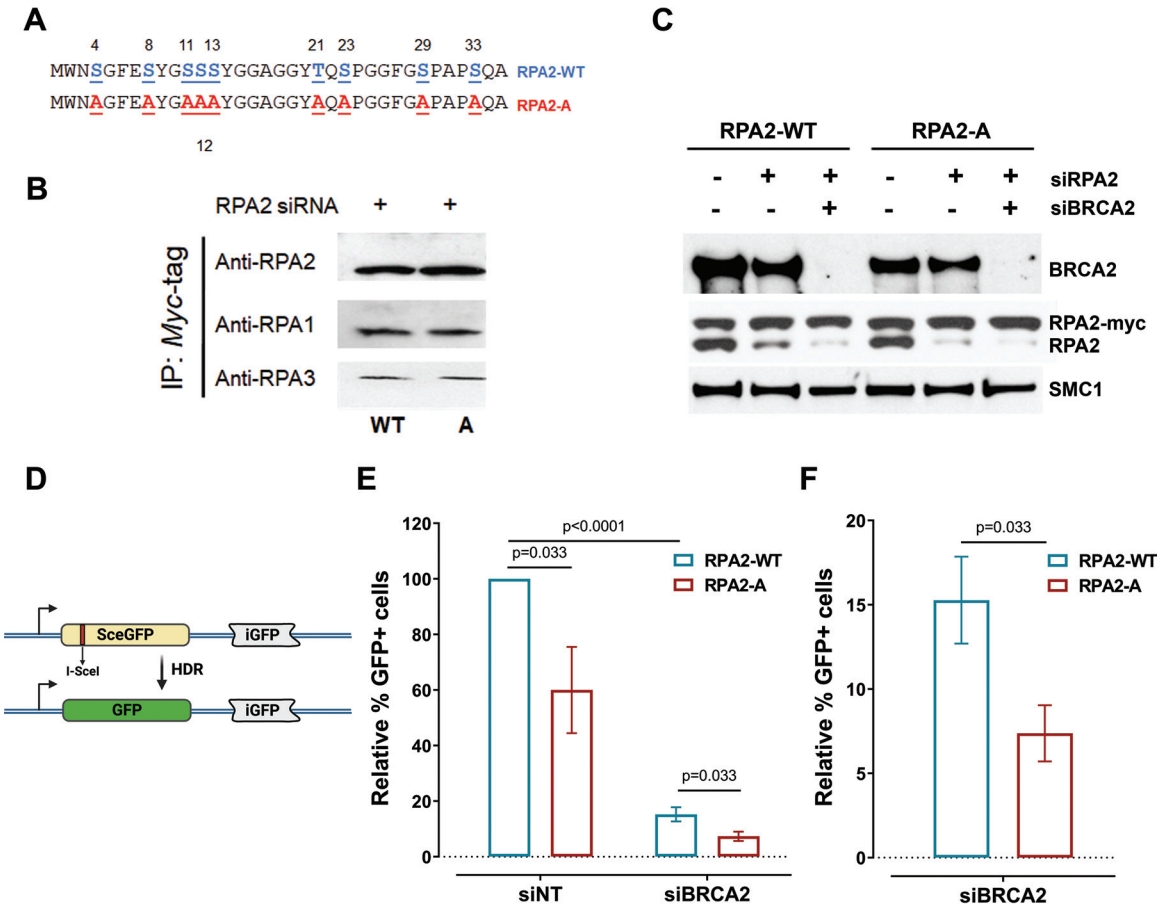

FIG 1 RPA phosphorylation is important for RAD52-dependent HR. (A) Schematic representation of RPA2 highlighting phosphorylation sites mutant in the N terminus of the phospho-dead protein (RPA2-A). Both contain a C-terminal Myc tag and were stably expressed in MCF7-DR-GFP cells. (B) IP pulldown with Myc antibody, showing RPA2-WT and -A. Exogenous proteins interact with RPA1 and RPA3. (C) MCF7 DR-GFP cells expressing RPA2-WT or phosphomutant RPA2-A were depleted of endogenous RPA2 by siRNA transfection along with siNT or siBRCA2. Western blots confirming depletion of BRCA2 and endogenous RPA2. (D) Schematic of the HR assay (DR-GFP). SceGFP is a full-length GFP gene disrupted by an I-SceI site. HR between SceGFP and the internal GFP (iGFP) fragment on the same plasmid upon I-SceI digestion restores GFP activity. (E) Forty-eight hours after siRNA treatment, MCF7 DR-GFP cells were transfected with the I-SceI endonuclease. Seventy-two hours after that, 10^5 cells per condition were tested by flow cytometry for expression of GFP. Experiments were normalized to RPA-WT siNT-treated cells. (F) siBRCA2 data, or RAD52-dependent HR events, plotted on different scales. Error bars represent standard errors of the means (SEM). $n = 5$ (a P value of <0.05 by t test was considered statistically significant).

MCF7 mammary adenocarcinoma cells stably expressing Myc-tagged RPA2 phosphorylation mutants were employed. These cells express either wild-type RPA2 (RPA2-WT), or a previously characterized RPA2 mutant with nine serine/threonine phosphorylation sites in the N-terminal domain mutated to alanine (RPA2-A), mimicking phosphorylation-defective RPA2 (Fig. 1A) (27, 28, 34). The stably expressed wild-type RPA2 (RPA2-WT) and RPA2-A mutant were expressed with a C-terminal Myc tag, while the endogenous RPA2 was depleted using small interfering RNA (siRNA) (Fig. 1C) to study the effects of the stably expressed RPA mutants specifically. As in previous studies, the RPA mutants maintained interaction with RPA1 and RPA3 (Fig. 1B) (27, 28). Each of these cell lines also contained the integrated DR-GFP construct to measure levels of gene conversion due to HR.

Consistent with earlier reports, cells expressing RPA2 phosphorylation mutants were observed to have reduced HR as measured by the DR-GFP assay (Fig. 1D and 1E; Table 1), confirming that RPA phosphorylation is important for HR (27, 30, 35). We further investigated the role of RAD52 in facilitating HR. Upon depletion of BRCA2 with siRNA (Fig. 1C), we observed a significant reduction in GFP expression levels corresponding to reduced HR activity (Fig. 1E). Previous studies using similar assays have shown that the remaining GFP expression is representative of DSB repair via HR and that RAD51 foci in these cells are dependent on RAD52 (13). Additionally, upon BRCA2 depletion, we also observed reduced

TABLE 1 Direct repeat recombinant frequencies

Assay and sample	% of GFP$^+$ cells	
	Avg	SD
DR-GFP		
siNT RPA2-WT	0.245	0.155
siNT RPA2-A	0.110	0.043
siBRCA2 RPA2-WT	0.032	0.015
siBRCA2 RPA2-A	0.017	0.013
SA-GFP		
siNT RPA2-WT	0.380	0.062
siNT RPA2-A	0.377	0.104

HR in the RPA phosphorylation-defective cell lines (RPA2-A) compared to RPA2-WT (Fig. 1E and 1F). Our data suggest that abrogation of RPA phosphorylation hampers not only BRCA2-dependent HR but also the RAD52-dependent pathway for repair of DSBs. Our experiments suggest that RPA phosphorylation facilitates RAD52-dependent HR.

RPA phosphorylation does not alter RAD52 biochemical activity. To investigate the role of RPA phosphorylation in facilitating RAD52-dependent HR, we studied the effects of RPA phosphorylation on its ability to bind ssDNA. We compared wild-type RPA protein to a hyperphosphorylated variant (pRPA) that was posttranslationally modified, using HeLa cell extracts, and purified. The phosphorylation status of RPA (Fig. 2A and B) was verified using antibodies specific to the S4/S8 epitope on RPA and

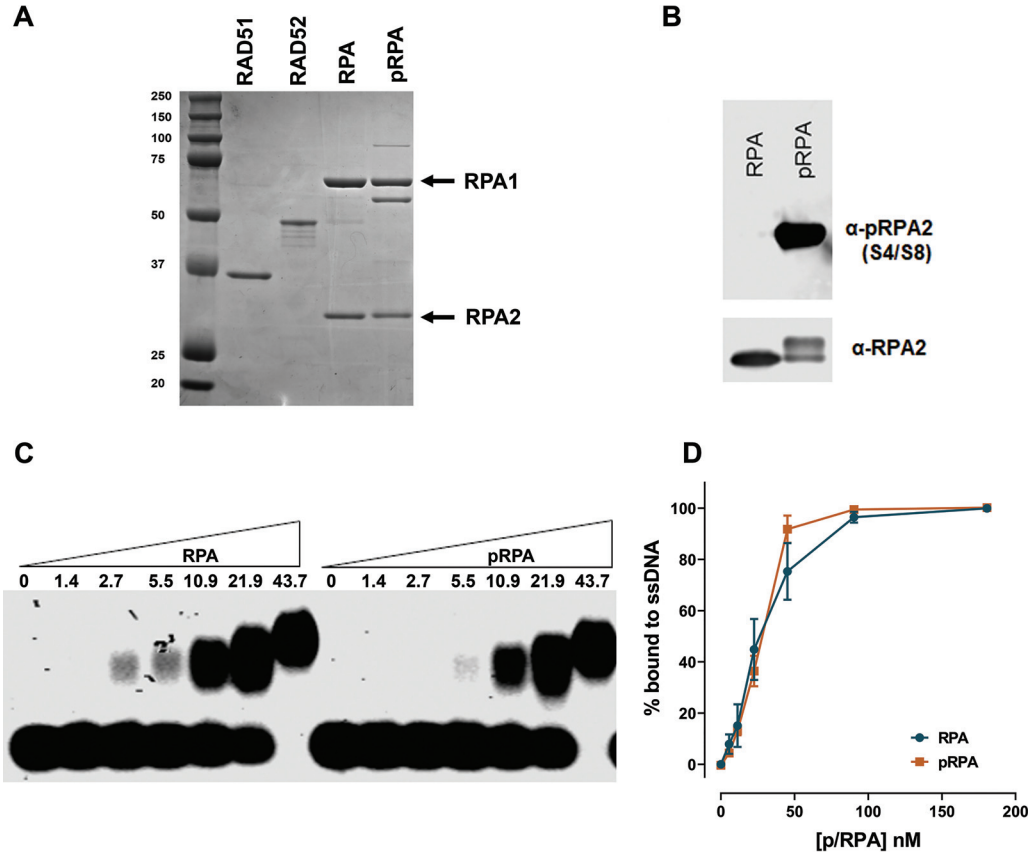

FIG 2 RPA phosphorylation does not affect DNA binding. (A) SDS-PAGE gel showing purified RAD52, RPA, and pRPA. (B) Western blots of purified RPA and pRPA used for the *in vitro* assays. (C) An ssDNA binding electrophoretic mobility shift assay (EMSA) was performed using RPA and pRPA. The proteins were incubated with an 80-nucleotide ssDNA oligonucleotide containing an infrared dye for 5 min, cross-linked with glutaraldehyde, run on an agarose gel, and imaged on a Li-Cor Odyssey machine. (D) Quantification of results in panel A. Bands were measured using Image Studio; points represent the percentage of ssDNA signal bound by protein as a fraction of the total of the signal in each lane (n = 3).

by an observed phosphorylation-dependent shift in mobility on immunoblotting. Using an *in vitro* RPA-ssDNA binding assay, we compared DNA binding activities of RPA and pRPA to 5 nM an 80-nucleotide ssDNA oligomer (400 nM nucleotide). We observed no significant difference in DNA binding between the two proteins: both proteins bound and saturated the ssDNA at the same concentration; in some cases either RPA or pRPA bound ssDNA at a slightly lower concentration, but this effect was not seen consistently and there was no significant difference (Fig. 2C and D).

In mammalian systems, RAD52 is known to predominantly catalyze single-strand annealing (SSA) as well as play a minor role in synthesis-dependent strand annealing (SDSA), both of which are critical in DSB repair. We postulated that RPA phosphorylation might affect RAD52 annealing activity. This notion was supported by previous evidence that RPA phosphorylation promotes RAD52-ssDNA contacts and the RPA-RAD52 interaction (36). To examine the effect of RPA phosphorylation on DNA strand annealing activity of RAD52, we designed strand annealing experiments based on those previously performed by Jensen et al. (6). Briefly, complementary ssDNAs were incubated separately with RPA or pRPA for 5 min, followed by incubation with RAD52 for 5 min. The two components were then mixed and further incubated to allow annealing. The reactions were at 1, 5, 15, and 30 min (Fig. 3A) (see Materials and Methods). RPA and pRPA on their own significantly reduced self-annealing of the substrates compared to the control with no RPA or RAD52 protein (Fig. 3C and D). This is expected, as in the cell, RPA binds ssDNA and prevents secondary structure formation while protecting nascent ssDNA from nuclease activity. When RAD52 was incubated without RPA or pRPA, most of the single-stranded substrates were annealed into the double-stranded product. (Fig. 3B and C, lanes 9 to 12). Adding RPA or pRPA before RAD52 inhibited RAD52 annealing, and there was no significant difference between the wild-type and phosphorylated RPA (Fig. 3B and C, lanes 1 to 4 versus 5 to 8). Thus, under our assay conditions, RPA phosphorylation did not promote RAD52 annealing *in vitro* (Fig. 3D).

To further investigate the effect of RPA phosphorylation on RAD52-dependent SSA *in vivo*, we used the cell-based SA-GFP assay, which consists of two *GFP* gene fragments, *5′GFP* and *SceGFP3′*, containing 266 bp of homology (Fig. 3E). Repair of a DSB in SceGFP3′, which is generated by I-SceI induction, results in a functional *GFP* gene as a result of SSA owing to the DNA strand from *SceGFP3′* annealing to the complementary strand of *5′GFP* (37). When either RPA2-WT or RPA2-A was overexpressed in cells containing the SSA reporter and depleted of endogenous RPA2, no observable difference was observed in the efficiency of SSA (Fig. 3E; Table 1) as measured by GFP-positive cells. This is consistent with our *in vitro* results suggesting that RPA2 phosphorylation status does not affect RAD52's ability to anneal single-stranded DNA.

RAD52-RPA interaction is unaffected by RPA hyperphosphorylation. To further characterize the role of RPA phosphorylation in regulating RAD52-dependent HR, we investigated the effect of RPA phosphorylation mutants on RAD52 recruitment to sites of DNA damage, since RAD52-dependent HR may be impaired in RPA phosphorylation-defective mutants due to a failure to recruit RAD52 to DSBs. As endogenous RAD52 foci are difficult to detect by immunofluorescence, RAD52 tagged with GFP was expressed in MCF7 cells expressing either the RPA-A mutant or RPA2-WT. Six hours after transfection, the cells were treated with 4 μM camptothecin (CPT) (or no treatment in control cells). The treated cells were then fixed and prepared for immunofluorescence imaging using confocal microscopy. The total number of foci per cell was scored (Fig. 4A and B), and the number of cells with more than five RAD52-GFP foci per condition were grouped as positive (Fig. 4C) events above background. After treatment with CPT, the difference in the number of RAD52-GFP foci observed between RPA2-WT and RPA2-A cells (Fig. 4B and C) was minimal. This suggests that upon DNA damage, RPA phosphorylation and dephosphorylation events do not significantly alter the recruitment of the RAD52 protein to DSBs. Either RAD52 is able to interact sufficiently with the RPA2 mutants for its recruitment, or RAD52 is recruited independently of RPA.

The interaction between RPA and RAD52 is well established, and it has been suggested to affect RAD52 function directly (22). Previous studies have also shown that RPA hyperphosphorylation promotes the interaction of RAD52 and RPA (36). These

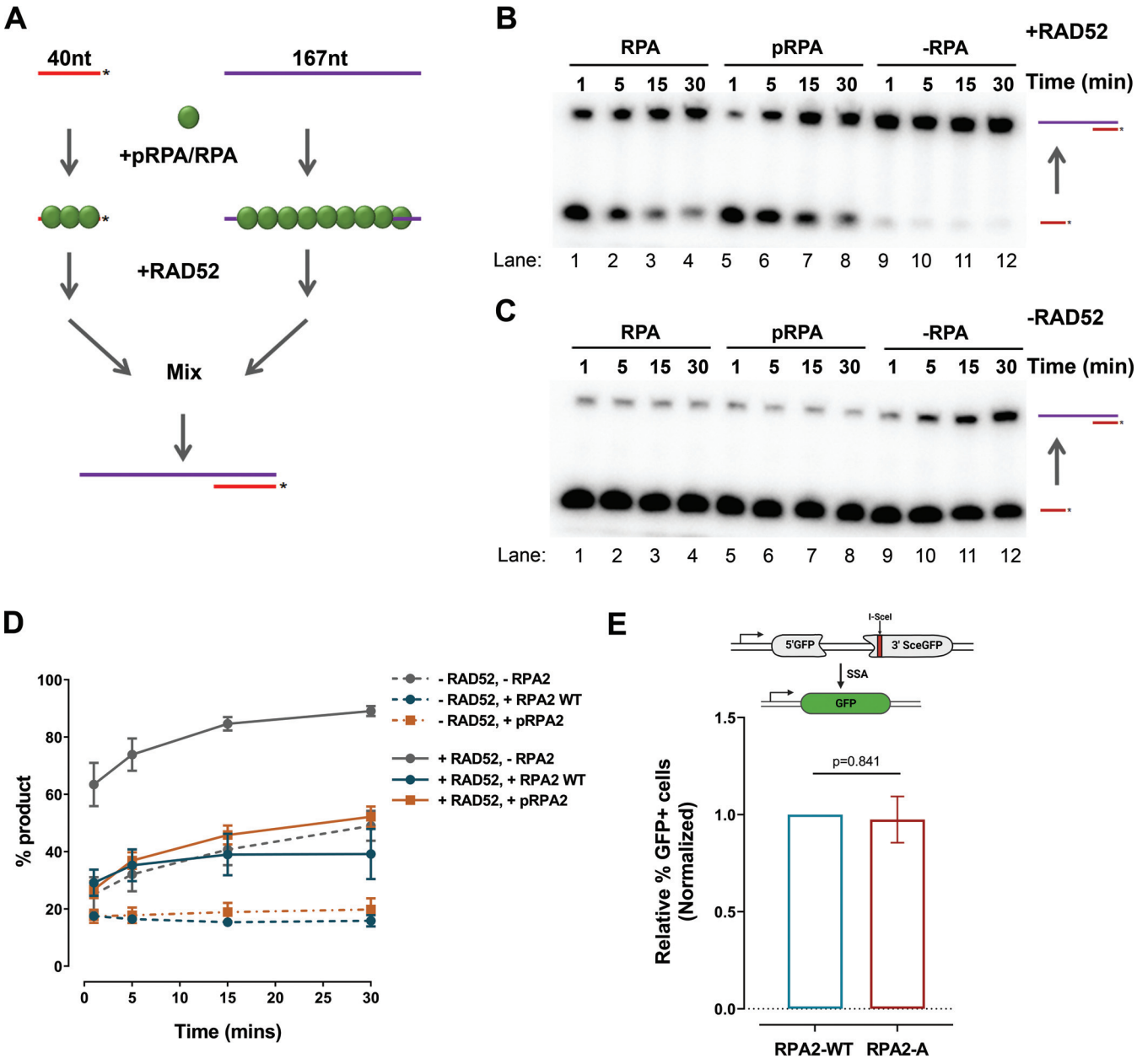

FIG 3 RPA phosphorylation does not affect RAD52-mediated strand annealing. (A) Schematic illustration of the strand annealing assay. Complementary ssDNAs in separate tubes were incubated with RPA, pRPA, or buffer for 5 min, RAD52 was added for 5 min, and then the ssDNAs were mixed. Aliquots were added to stop buffer at 1, 5, 15, and 30 min, run on a polyacrylamide gel, and imaged on a phosphorimager. (B and C) Autoradiograms of reaction described for panel A. (D) Bands in panels B and C were quantified, and the signal of the annealed product as a percentage of the total signal in each lane was determined and plotted ($n = 3$). (E) Schematic of the single-strand annealing assay (SA-GFP). 5′ GFP and 3′ SceGFP are GFP fragments bearing 266 bp of homology. Single-strand annealing repair of the I-SceI-induced DSB generates a functional GFP gene. Forty-eight hours after treatment (siRNA and RPA2 overexpression), U2OS-SA-GFP cells were transfected with the I-SceI endonuclease. Seventy-two hours after that, 100,000 cells per condition were tested by flow cytometry for expression of GFP. Experiments were normalized to RPA-WT-treated cells ($n = 3$). Error bars represent SEM (a P value of <0.05 by t test was considered statistically significant).

prior studies possibly explain the differences we observe between RPA2-WT and RPA-phosphomutant cells in RAD52-dependent HR and RAD51 foci. We further investigated the effect of RPA phosphorylation on the interaction between RAD52 and RPA. Using immunofluorescence experiments, the colocalization between RPA2-Myc-tagged proteins and RAD52-GFP foci (Fig. 4D and E) was measured using Pearson's coefficient of colocalization. We also determined the percentage of cells that had RAD52-GFP foci in which at least five of those foci were colocalized with RPA (Fig. 4D to G). RPA2 colocalized with RAD52-GFP at similar levels in RPA2-WT and RPA-A cells in untreated cells and after treatment

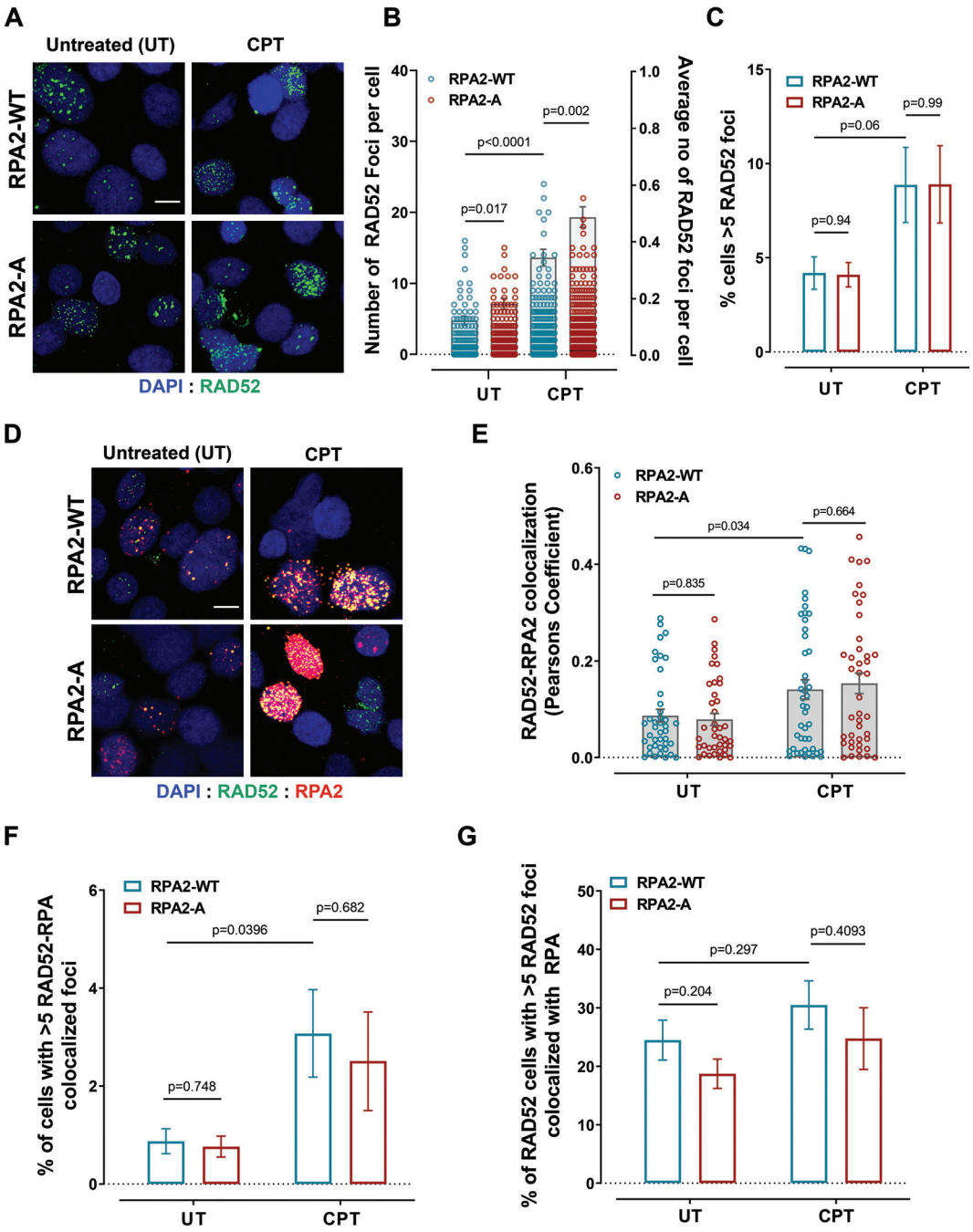

FIG 4 RAD52 recruitment after damage is unaffected by RPA phosphorylation status. MCF7 cells expressing RPA2-WT or phosphomutant RPA2 (RPA2-A) were depleted of endogenous RPA2 by electroporation of siRPA, and RAD52-GFP was expressed. Forty-eight hours later, cells were plated on glass slides. The next day, cells were treated with CPT for 6 h, then fixed with formaldehyde, and permeabilized with Triton X-100. Cells were stained with Myc primary antibody and fluorescent secondary antibody and then imaged on a confocal microscope. (A) Representative images of RAD52 foci across the different conditions; data are quantified in panel B. (B) Total number of RAD52 foci per cell plotted (left *y* axis) and the average number of RAD52 foci per cell (right *y* axis). Each dot represents the focus count of one nucleus. More than 2,500 cells were scored for each condition. (C) Additionally, 300 cells were counted manually per condition in each experiment, and cells with >5 RAD52-GFP foci were counted as positive for RAD52. (D) Representative images for RAD52-RPA2 colocalizing foci across the different conditions; data are quantified in panels E and F. (E) Pearson's coefficient for RAD52-RPA2 colocalization was calculated using ImageJ and plotted. Each dot represents the correlation coefficient of one imaging field. (F) Cells with >5 RAD52-GFP foci colocalized with RPA2-Myc were manually counted as positive for colocalization in at least 300 cells. (G) Percentages of cells with RAD52-GFP in which >5 of those foci are colocalized with RPA2-Myc ($n = 3$). Bars, 10 μm. Error bars represent SEM (a P value of <0.05 by t test was considered statistically significant).

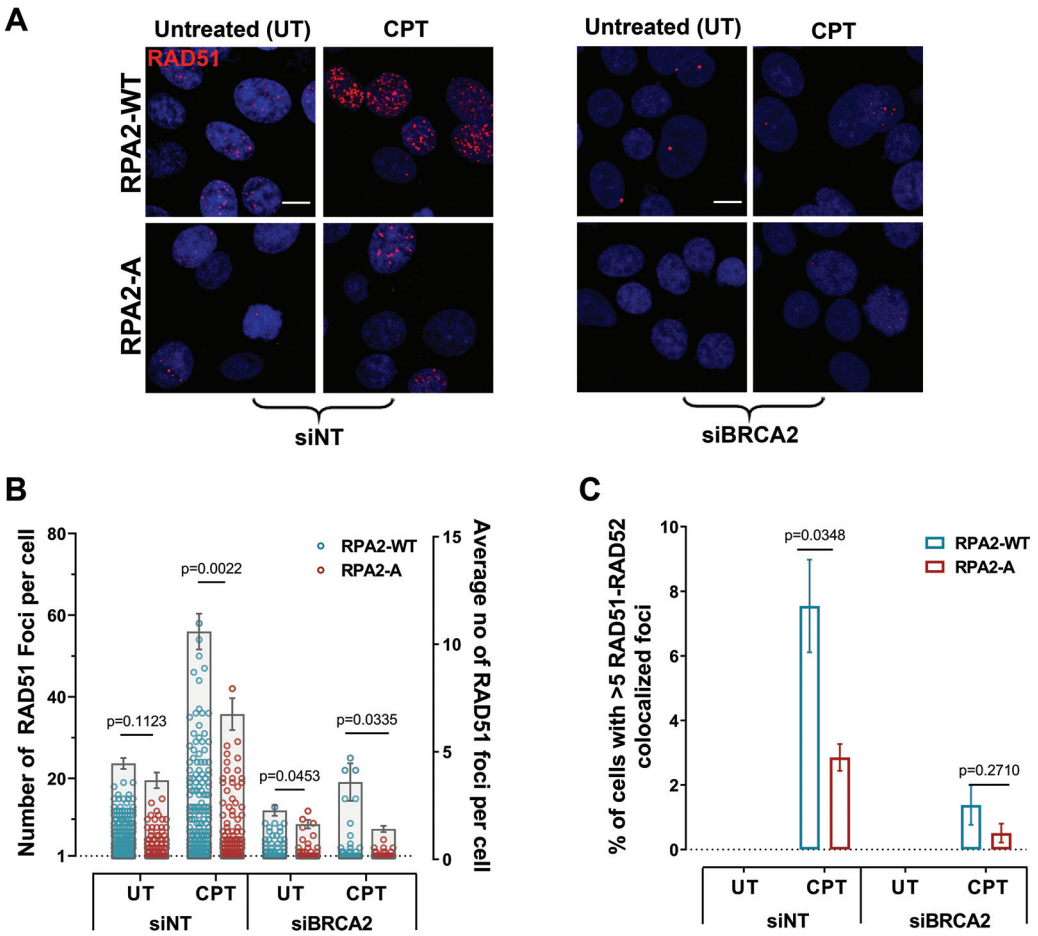

FIG 5 RPA phosphorylation is important for RAD51 foci formation in response to DNA damage. MCF7 cells expressing RPA2-WT or phosphomutant RPA2 (RPA2-A) were depleted of endogenous RPA2 by electroporation of siRPA2, and RAD52-GFP was expressed. Forty-eight hours later, cells were depleted of BRCA2 by Lipofectamine RNAiMax transfection of siBRCA2. Twenty-four hours after that, cells were plated on glass slides. The next day, cells were treated with CPT for 4 h, then fixed with formaldehyde, and permeabilized with Triton X-100. Cells were stained with RAD51 primary antibody and fluorescent secondary antibody and then imaged on a confocal microscope. (A) Representative images of RAD51 foci across the different conditions. Data are quantified in panel B. (B) Total number of RAD51 foci per cell (left *y* axis) and average number of RAD51 foci per cell (right *y* axis). Each dot represents the focus count of one nucleus. All cells containing more than 1 RAD51 focus was included in the analysis, and >700 cells were scored for each condition. (C) Three hundred cells were manually counted per condition in each experiment, and cells with >5 RAD51 foci were counted as positive for RAD51 ($n = 3$). Bars, 10 μm. Error bars represent SEM (a P value of <0.05 by t test was considered statistically significant).

with CPT. Our results suggest that RPA phosphorylation has minimal impact on the interactions between RPA and RAD52.

RPA hyperphosphorylation is essential for RAD51-RAD52 interaction. From the data above, it was apparent that, although RAD52 forms foci in RPA phosphorylation mutants, the RPA phosphorylation status seems to have a profound impact on RAD52-dependent HR (Fig. 1 and 4). In wild-type HR-proficient cells, the RAD51 recombinase is recruited to DSBs in response to DNA damage. The accumulation of RAD51 protein at these DSBs can be visualized as punctate foci by immunofluorescence. Furthermore, the levels of RAD51 foci are significantly reduced in cells that have impaired HR. To investigate if the effect of RPA phosphorylation on RAD52-dependent HR was a function of the inability of RAD52 to recruit RAD51 normally in the absence of RPA hyperphosphorylation, we quantified RAD51 focus formation. DSBs were induced by treating MCF7 cells for 4 h with 4 μM CPT. RAD51 foci were visualized by immunofluorescence, and the total number of foci per cell was determined (Fig. 5A and B). Additionally, the percentages of cells with more than five RAD51 foci were grouped as positive HR events above background (Fig. 5C). In cells treated with

nontargeting siRNA with BRCA2-dependent RAD51 recruitment intact, we observed a dependence of RAD51 recruitment on RPA phosphorylation, i.e., RPA2-A cells displayed reduced RAD51 foci in both untreated cells and cells treated with CPT compared to RPA2-WT cells, in agreement with previous reports that RPA phosphorylation is important for RAD51 recruitment and HR (Fig. 5B and C). In cells depleted of BRCA2, where RAD51 focus formation is dependent on RAD52, RAD51 foci were significantly reduced in the RPA2-A cells compared to RPA2-WT cells.

To investigate why RAD52 is more efficient at HR and RAD51 recruitment in RPA2-WT than RPA2 phosphorylation-defective cells (RPA2-A), we measured Pearson's coefficient of colocalization in MCF7 cells expressing RAD52-GFP with RAD51. Upon induction of DNA damage, RAD52-GFP colocalized with RAD51 at significantly higher levels in the RPA2-WT line than in the RPA2-A line, with and without BRCA2 (Fig. 6A to E). Furthermore, the percentage of cells with RAD52-GFP foci that are colocalized with RAD51 was lower in RPA2-A cells than RPA2-WT cells (Fig. 6D). Additionally, in unperturbed cells, we did not observe any RAD52-RAD51 colocalization above the background threshold of five colocalized foci (Fig. 6C and E). Taken together, our observations suggest that RPA phosphorylation is necessary for RAD52-dependent recruitment of RAD51 and subsequent HR, but it does not affect RAD52's annealing ability at a DSB (Fig. 7).

DISCUSSION

In *Saccharomyces cerevisiae*, Rad52 functions as a critical mediator of HR by facilitating the loading of Rad51 onto ssDNA. However, in mammalian systems and other vertebrates, BRCA2 is known to function as the primary mediator of RAD51 filament formation (6, 7), while prior studies have shown a limited role for RAD52 in HR. Additionally, loss of RAD52 has little consequence for cell viability (10, 11, 37), raising questions regarding its function in mammalian cells. Recent evidence suggests that RAD52 may provide an alternative mediator pathway to BRCA2 function (12, 13). We have previously shown that cells lacking both BRCA2 and RAD52 have increased chromosomal instability, pointing to a severe HR deficiency and a role for RAD52 in RAD51-mediated HR in BRCA2-deficient cells (13). RAD52 is also synthetically lethal with BRCA1 and PALB2 (38), as RAD51 recruitment and focus formation are dependent on RAD52 in BRCA1- and PALB2-depleted cells (38). RAD52 is also synthetically lethal with XRCC3 (39). BRCA2 is epistatic to RAD51 paralogs in response to DNA damage, as measured by cellular survival after treatment with DNA-alkylating agents (40), and synthetically lethal with RAD52 in human cells (41). Several lines of evidence suggest that the RAD52 backup pathway functions independently of the BRCA pathway, where RAD52 accumulation to DNA damage sites and colocalization with RPA2 are not affected by BRCA2 status (13). Additionally, recent studies have shown that RAD52 can load RAD51 at replication-associated one-ended DSBs (42) and that RAD52 can interact with PALB2 independently of BRCA2 (43), further supporting the idea that RAD52 can help mediate RAD51 filament formation in BRCA2-deficient cells.

In this study, we investigated the biological consequences of RPA phosphorylation on RAD52 mediator function. RPA hyperphosphorylation serves a critical function for the repair of DSB through HR by signaling the recruitment of several proteins that mediate the HR pathway. RPA hyperphosphorylation is also an important marker for repair of replication-associated DNA breaks via HR. In mammalian cells, defects in RPA phosphorylation induce sensitivity to DNA-damaging agents (27, 29, 30), which lead to persistent DNA breaks (27, 29, 44, 45). While phosphorylation-defective RPA mutants can associate with DNA damage sites (28), the recruitment of downstream factors in the HR pathway is severely impaired, supporting a model where RPA can localize to breaks and sites of stress without phosphorylation.

Using the DR-GFP assay, we verified the role of RPA phosphorylation in HR and observed that gene conversion events were significantly reduced in phosphorylation mutants (Fig. 1). Reduced gene conversion events have been associated with aberrant sister chromatid exchanges, which are increased in phosphorylation mutants (46). Additionally, phosphorylated RPA has been shown to inhibit resection *in vitro*,

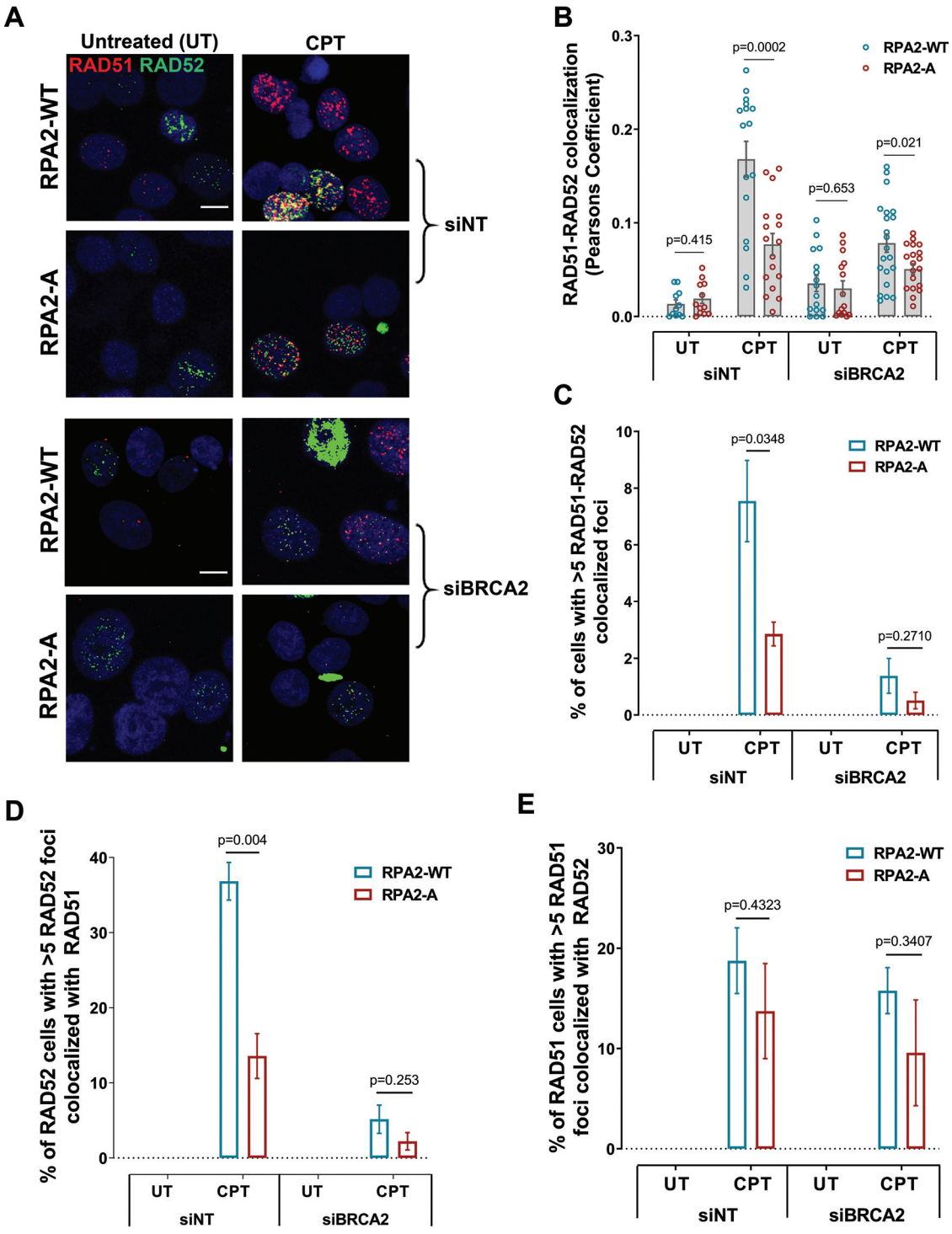

FIG 6 RPA phosphorylation is important for RAD52-dependent RAD51 foci. MCF7 cells expressing RPA2-WT or phosphomutant RPA2 (RPA2-A) were depleted of endogenous RPA2 by electroporation of siRPA2, and RAD52-GFP was expressed. Forty-eight hours later, cells were depleted of BRCA2 by Lipofectamine RNAiMax transfection of siBRCA2. Twenty-four hours after that, cells were plated on glass slides. The next day, cells were treated with CPT for 4 h, then fixed with formaldehyde, and permeabilized with Triton X-100. Cells were stained with RAD51 primary antibody and fluorescent secondary antibody and then imaged on a confocal microscope. (A) Representative images for RAD51-RAD52 colocalizing foci across the different conditions. Data are quantified in panels B and C. (B) Pearson's coefficient for RAD51-RAD52 colocalization was calculated using ImageJ and plotted. Each dot represents the correlation coefficient of one imaging field. (C) Three hundred cells were counted per condition in each experiment, and cells with >5 RAD51 foci colocalized with RAD52-GFP were counted as positive for colocalization. (D) Percentage of cells with RAD52-GFP foci in which >5 of those foci colocalized with RAD51. (E) Percentage of cells with RAD51 foci in which >5 of those foci colocalized with RAD52-GFP (n = 3). Bars, 10 μm. Error bars represent SEM (a P value of <0.05 by t test was considered statistically significant).

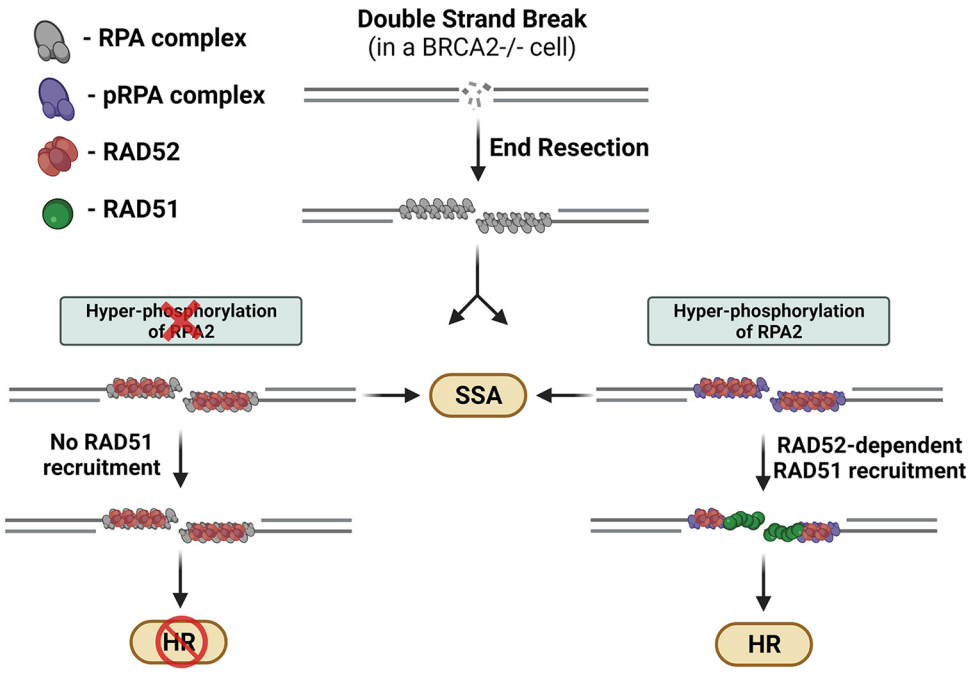

FIG 7 RPA phosphorylation is essential for RAD52-dependent HR in BRCA2$^{-/-}$ cells. Upon DNA damage, the broken DNA ends are processed and resected by exonucleases, followed by the loading of the RPA complex (gray). In BRCA2$^{-/-}$ cells, RAD52 (red) is loaded onto the RPA-coated ends and the cell proceeds toward RAD51 loading (green) and repair via HR. If the RPA2 hyperphosphorylation (purple) is hindered, the cell still efficiently loads RAD52 but is unable to carry out RAD51 loading and HR. In either case, RPA hyperphosphorylation does not affect RAD52-dependent SSA.

suggesting a feedback loop between DNA resection and the DNA damage response (47). This is primarily due to impaired interactions with HR and DNA damage response proteins, including MRN (33, 48), p53 (35, 49), RAD51 (30, 35, 36), PALB2 (50), and ATR (36). Thus, RPA phosphorylation is important for the BRCA-dependent DNA repair pathway.

The effect of RPA phosphorylation on the RAD52 mediator pathway has been poorly characterized. Other groups have established that RPA phosphorylation improves its interaction with RAD52 (36). Phosphorylated RPA colocalizes with RAD52 in foci and stabilizes the RPA-ssDNA-RAD52 complex (36). Furthermore, cross-linking experiments have shown increased RAD52-ssDNA interactions when the RPA in the complex is hyperphosphorylated (31). Our data obtained with cells supports this evidence that RPA phosphorylation promotes RAD52 function as an alternative mediator. We showed that RAD52-dependent HR, as measured by RAD51 foci and the DR-GFP assay, is dependent on functional phosphorylation of RPA even after depletion of the canonical BRCA2 mediator protein (Fig. 1 and 5). This supports the importance of RPA and its phosphorylation in both the BRCA and RAD52 pathways of HR.

We have shown that RPA phosphorylation promotes the association of RAD51 and RAD52 by colocalization, as RAD51 and RAD52 colocalize at considerably higher levels in RPA2-WT cells than in RPA2-A mutant cells. We also show that the association of RAD51 and RAD52 is DNA damage dependent, which supports a role for RAD52 in facilitating RAD51 nucleoprotein formation in DNA repair. Assuming that RAD52 serves as a backup for BRCA2 in facilitating RAD51 nucleoprotein formation, we expected that the extent to which RAD52 colocalizes with RAD51 would increase when BRCA2 is depleted. However, the lack of such an observation suggests that while in normal cells, a fraction of RAD51 recruitment to resected DNA is due to RAD52 mediator function, and the absence of BRCA2 does not enhance its mediator activity, supporting the independence of RAD52 from the BRCA pathway. In both BRCA2-proficient and BRCA2-depleted cells, the percentage of cells with RAD52 foci that colocalize with RAD51 was reduced in RPA2-A phosphomutant cells compared to RPA2-WT cells. Combining our observations showing fewer RAD52-dependent (in BRCA2-depleted cells)

RAD51 foci (Fig. 5 and 6) and reduced RAD52-dependent HR in RPA2-phosphomutant cells (Fig. 1) leads us to suggest that RPA phosphorylation promotes RAD52-dependent RAD51 recruitment. Taken together, these data show that RPA phosphorylation is an important regulator of RAD52 mediator function, although the exact mechanism is yet to be determined.

The effects of RPA phosphorylation on RAD52 function *in vitro* have been largely unresolved. Several prior studies have suggested that the interaction of RPA and RAD52 is improved with RPA phosphorylation (36), phospho-RPA promotes RAD52 contacts with ssDNA in RPA-RAD52-ssDNA complexes (31), and the interaction between RPA and RAD52 is functionally significant, since RAD52 mutants that do not interact with RPA fail to enhance HR in monkey cells in contrast to RAD52-WT cells (22). The RAD52-RPA interaction facilitates binding of RAD52 to RPA-ssDNA, and this interaction is necessary for RAD52 to counteract RPA's helix-destabilizing activity (51, 52).

Biochemically, RAD52 has been shown to have strand-annealing activity and RAD51 mediation activity in the absence of RPA or under suboptimal conditions for RAD51, but it has not been shown to displace RPA from ssDNA to allow RAD51 filament formation (6). Additionally, recent studies employing DNA curtains have shown that though RAD52 by itself cannot remove RPA from ssDNA, and addition of RAD51 to the reaction mixture leads to complete dissociation of the RPA-RAD52 complex followed by RAD51 nucleoprotein filament formation (52). Using DNA binding and strand annealing experiments, we observed that RPA phosphorylation does not promote RAD52 DNA binding or annealing activities *in vitro*. No effect of RPA phosphorylation was observed in SSA-based GFP reporter assays (Fig. 3).

It is possible that additional factors are needed and/or the physiological conditions in cells are required to demonstrate a role of RPA phosphorylation in promoting RAD52 annealing activity. Previous reports have shown that the protein DSS1 and not the phosphorylation cycle of RPA helps promote RAD52's observed DNA repair activity. The DSS1-RAD52 interaction facilitates repair by altering the RAD52 conformation and aiding its release from the DNA end (53). Our results indicate that RPA phosphorylation has a minimal effect if any on RAD52 functions in the cell that rely on its DNA binding or annealing activity. The interactions between RAD52 and RPA in the absence of phosphorylation are significantly reduced, as previously demonstrated in immunoprecipitation experiments (36), potentially being facilitated by a weak interaction between RAD52 and RPA1 (54–56), suggesting that our observations of diminished RAD52-dependent HR in phosphorylation mutants could have been due to impaired interactions between RAD52 and RPA. Paradoxically, RAD52 foci form normally in RPA phosphorylation mutant cells after damage (Fig. 4). Given our observation that RPA phosphorylation promotes RAD52-dependent HR and improved interaction with RAD52, it is possible that, although RAD52 is recruited to foci independently of RPA phosphorylation, either through its interactions with RPA2 and RPA1 or through its own DNA binding activity, the association between RAD52 and RPA is not efficient without phosphorylation of RPA32. Alternatively, the lack of cycling between phosphorylation and dephosphorylation prevents a hand-off of tighter ssDNA contacts from RPA to RAD52, thereby causing defective HR.

Taken together, our data suggest that in the absence of RPA phosphorylation, it is not the reduced association between RAD52 and RPA but the failure of RAD52 to recruit RAD51 that leads to the failure to promote HR in BRCA2-depleted cells. The role of RAD52 in BRCA-proficient cells is an interesting question. Despite RAD52's lack of severe HR phenotype, there are some recombination phenotypes of RAD52, suggesting that RAD52 does play a role even in BRCA-competent cells (11, 13, 57–59). RAD52 interacts with RAD51 and RPA (15, 22, 54, 58, 60–64), and its synthetic lethality with DNA repair factors suggests that it plays an important role in HR. The DNA annealing activity of RAD52 may play a role in BRCA-proficient cells, through SSA, second-end capture, or synthesis-dependent strand annealing (51, 65–68).

In cancer patients carrying *BRCA* mutations only, tumor cells are BRCA deficient (usually heterozygous $BRCA^{mut/-}$), while normal cells are proficient in HR, containing one functional and one nonfunctional copy of *BRCA1* or *BRCA2*. Thus, targeting a protein such as RAD52, which is synthetically lethal only with biallelic BRCA2 deficiency, would result in selective death of tumor cells. The synthetic lethal relationship between poly(ADP-ribose) polymerase

(PARP) and BRCA—believed to underlie the effectiveness of treatment of BRCA-deficient cancers by PARP inhibitors—provides a proof of principle that synthetic lethality can be exploited to develop cancer therapeutics. RAD52 loss or inhibition may have advantages over PARP inhibitors in that it causes little DNA damage in wild-type cells, making the target attractive for cancer treatment. Our work demonstrates that RPA phosphorylation is important not only for the BRCA pathway but also for the RAD52 pathway, making this interaction a potential therapeutic target.

Our data support a model of RAD52-dependent HR that is promoted by hyperphosphorylation of RPA (Fig. 7). After a DSB or replication fork collapse, the ends are resected to generate 3′ ssDNA overhangs that are bound by RPA, which is then hyperphosphorylated. RAD52 is recruited to the damage site by RPA regardless of RPA phosphorylation status. However, RPA phosphorylation enhances its interactions with RAD52, augmenting recruitment of RAD51 and promoting nucleoprotein filament formation. RAD51 then catalyzes homology search and strand invasion, promoting HR. Meanwhile, the other functions that RAD52 has in DSB repair via strand annealing activity remain unaltered. The exact mechanism by which RAD52 mediates HR needs to be investigated further. The role of cycling phospho-RPA and other factors needed to regulate RAD52-mediated HR still remains undetermined.

MATERIALS AND METHODS

Cell lines. Myc-tagged RPA2 expression vectors were electroporated into MCF7 cells, a breast adenocarcinoma cell line, containing the DR-GFP reporter construct. Cells were grown in blasticidin, and resistant colonies were expanded and tested for expression of RPA-mutant cell lines. Cells were maintained in Dulbecco's modified Eagle medium (DMEM) with 100 U/mL penicillin, 100 μg/mL streptomycin, 10% bovine growth serum (BGS), 20 mM HEPES. NaOH (pH 7.4), and 15 μg/mL blasticidin. RPA2-WT and RPA2-A plasmids were generated from pEF6 by insertion into the XbaI and BstBI sites of the pEF6/Myc-HisA vector (Invitrogen). Expression of the 6-His tag from pEF6/Myc-HisA was prevented by mutating the ATG codon at position 1863 to a TGA codon.

siRNA. siRNAs were obtained from Horizon Discovery (Dharmacon). siRPA was two ON-TARGETplus (Horizon Discovery; custom siRNA) sequences mixed in equal amounts (sense sequence: AAC UGG AUC UAA CUG GGU ACC UU; GCU UCU AGG AAG UAG GUU UCA UU). siBRCA2 was an ON-TARGETplus SMARTpool (L-003462-00) (target sequences: GAA ACG GAC UUG CUA UUU A, GGU AUC AGA UGC UUC AUU A, GAA GAA UGC AGG UUU AAU A, and UAA GGA ACG UCA AGA GAU A). siNT was an ON-TARGETplus SMARTpool (D-001810-10) (target sequences: UGG UUU ACA UGU CGA CUA A, UGG UUU ACA UGU UGU GUG A, UGG UUU ACA UGU UUU CUG A, and UGG UUU ACA UGU UUU CCU A).

Cell-based DNA repair assays. MCF7-pDR-GRP cells containing stably integrated Myc-tagged RPA2, either WT or RPA2-A, were assayed for gene conversion events as previously described (32). One million cells were transfected with 2 μg each siRPA and siBRCA2 (or siNT control) using the Amaxa electroporation system. Forty-eight hours later, 2 μg of the pCMV-ISceI-3xNLS plasmid along with 0.5 μg of each siRNA was transfected using the Lipofectamine 2000 reagent (Life Technologies). Seventy-two hours later, the cells were harvested, and percentages of GFP-positive cells per 100,000 cells were determined by flow cytometry (FACSCalibur; Becton Dickinson).

U2OS-SA-GFP cells were assayed for single-strand annealing events as previously described (37). 1 million cells were transfected with 2 μg each siRPA and RPA2-WT- or RPA2-A-expressing plasmid using the Amaxa electroporation system. Forty-eight hours later, 2 μg of the pCMV-ISceI-3xNLS plasmid along with 0.5 μg of each siRNA was transfected using the Lipofectamine 2000 reagent (Life Technologies). Seventy-two hours later, the cells were harvested, and percentages of GFP-positive cells per 100,000 cells were determined by flow cytometry (FACSCalibur; Becton Dickinson).

Preparation of protein lysates for immunoblotting. Cells were trypsinized and pelleted by centrifugation followed by lysis using radioimmunoprecipitation assay (RIPA) buffer containing 1× protease inhibitor cocktail (Halt protease inhibitor cocktail; Thermo Scientific) and incubated on ice for 5 min. Lysates were sonicated, incubated on ice for 30 min, and then centrifuged at a relative centrifugal force (RCF) of 16,100 for 20 min. Protein concentrations in the lysates were determined by using Bio-Rad protein assay dye reagent concentrate and comparing against a bovine serum albumin (BSA) protein standard curve, measured on a Tecan Infinite M200 reader.

Western blots. Twenty to one hundred micrograms of protein lysates was loaded onto precast gels from Life Technologies (NuPAGE Novex 10% bis-Tris SDS-PAGE gels were run in NuPAGE MOPS [morpholinepropanesulfonic acid] SDS running buffer for all proteins except BRCA2; 3 to 8% Tris-acetate gels run in NuPAGE Tris-acetate running buffer were used for BRCA2 and SMC-1) in a Novex mini-cell or midi apparatus at 110 V for 2 h. Gels were then transferred onto nitrocellulose membranes using transfer buffer (1.4% glycine, 0.3% Tris base, 20% methanol) at 40 V overnight in a Mini-PROTEAN Tetra system (Bio-Rad). Membranes were stained with Ponceau S solution to verify even transfer and then blocked in 5% milk in TBS-T (Tris-buffered saline with 0.1% Tween) or Odyssey TBS blocking solution for 1 h. Membranes were incubated in primary antibodies diluted in 5% milk TBS-T (2.5% for BRCA2) or Odyssey TBS blocking solution with 1% Tween overnight. Antibody was removed, and the membrane was washed 3 times for 10 min in TBS-T. Membranes were then incubated with secondary antibodies for 1 h and washed again 3 times with TBS-T. Membranes incubated with horseradish peroxidase (HRP)-

conjugated secondary antibodies were incubated in Western Lightning Plus-ECL (Perkin Elmer) for 5 min and then exposed to autoradiography film. Membranes incubated in IRDye secondary antibodies were imaged on the Odyssey CLx System (Li-Cor).

Antibodies. Antibodies used for immunoblotting included those against RPA2 (cell signaling RPA2 [4E4] rat monoclonal antibody [MAb]; no. 2208), 1:1,000; pRPA (Abcam anti-RPA32/RPA2 [phospho S4 + S8] antibody [ab87277]), 1:400; Myc (cell signaling Myc rabbit [rb] polyclonal antibody; no. 2272), 1:400; Myc (Myc-Tag [9B11] mouse MAb; no. 2276), 1:1,000; RAD52 (rb polyclonal RAD52 antibody H-300; sc-8350); RAD52 (mouse monoclonal Rad52 antibody F-7; sc-365341); BRCA2 (BRCA2 mouse MAb; OP-95; EMD Millipore); SMC-1 (rabbit polyclonal; Bethyl Laboratories); and actin (mouse monoclonal; EMD Millipore; MAB1501). Secondary antibodies included Pierce goat anti-mouse and goat anti-rabbit HRP-conjugated IgG, Li- or IRDye-conjugated 800CW goat anti-mouse IgG, IRDye-conjugated 800CW goat anti-rabbit IgG, and IRDye-conjugated 800CW goat anti-rat IgG.

Antibodies used for immunofluorescence include those against Myc (Myc-Tag [9B11] mouse MAb; no. 2276) and RAD51 (rabbit monoclonal, Abcam; ab133534), 1:2,500. The secondary antibodies were Alexa Fluor 568-conjugated goat anti-mouse immunoglobulin (Life Technologies) and Alexa Fluor 555-conjugated goat anti-rabbit immunoglobulin.

Immunoprecipitation. Nuclear lysates were collected using the universal magnetic coimmunoprecipitation (co-IP) kit (Active Motif). A protein A/G SpinTrap buffer kit (GE Healthcare) was used to immunoprecipitate proteins as follows. Protein A magnetic Sepharose beads (GE Healthcare) were equilibrated by resuspension in 500 μL binding buffer, which was then removed. Beads were incubated with 10 μg primary antibody (Myc mouse; Cell Signaling no. 2276) for 4 h. They were washed in 500 μL binding buffer and then in cross-link solution A. The beads were cross-linked to the primary antibody twice in 500 μL cross-link solution A with 50 mM dimethyl pimelimidate (DMP) for 30 min, with a wash in cross-link solution A between. After cross-linking, the beads were washed in 500 μL cross-link solution A. They were blocked for 15 min in cross-link solution B, and unbound antibody was then eluted for 10 min at 50°C in elution buffer. Antibody-cross-linked beads were washed twice in 500 μL wash buffer, and then nuclear lysates were added to the beads and incubated for 3 h. Unbound lysates were removed, and the antibody- and protein-bound beads were then washed twice with wash buffer. Bound protein was eluted in twice for 10 min in elution buffer. The eluate was concentrated using Amicon Ultra 0.5-mL centrifugal filters (Ultracel 10K; Millipore) and run on Western blots as described above. Binding and wash buffer (50 mM Tris, 150 mM NaCl [pH 7.5]), elution buffer (0.1 M glycine-HCl [pH 2.9]), cross-link solution A (200 mM triethanolamine [pH 8.9]), and cross-link solution B (100 mM ethanolamine [pH 8.9]) were used.

Confocal microscopy and immunofluorescence. Cells were simultaneously fixed and permeabilized in 0.5% Triton X-100 and 0.5% paraformaldehyde diluted in phosphate-buffered saline (PBS) for 15 min. They were then blocked at 4°C overnight in 5% BGS in PBS. The following morning, they were incubated in primary antibody for 3 h at room temperature. Cells were washed 3 times for 5 min in 0.5% Triton X-100 in PBS and then incubated in secondary antibody for 1 h. Cells were washed again 3 times for 5 min in 0.5% Triton X-100 in PBS. Mounting medium with DAPI (4′,6-diamidino-2-phenylindole; Vectashield) was added, and then coverslips were added. Cells were imaged on a Zeiss LSM-510 confocal microscope. Images were further processed and analyzed using ImageJ2 (69).

Confocal image analysis. Figures were analyzed using a batch script. Automated focus counting for RAD52 (Fig. 4B) and RAD51 (Fig. 5B) were performed on maximum-intensity Z projections using a custom-written ImageJ macro. Cell nucleus and focus segmentation was performed with a series of auto-thresholds and watershed algorithms (ImageJ plugin) on the 8-bit images (split into its constituent channels) of either the nucleus background or the focus signal. Data analysis was performed with the particle analyzer (ImageJ plugin). Pearson's coefficient was calculated using the JACoP plug-in (70) in ImageJ2, where channel A was assigned to the 488-nm excitation and channel B corresponded to 561-nm excitation. For Fig. 4E, the channel A and B thresholds were set at 115 and 110, respectively, while they were fixed at 73 and 43 for Fig. 6B.

Purification of proteins. RPA and phosphorylated RPA were purified in Gloria Borgstahl's lab as described previously (31, 71). To generate phosphorylated RPA, RPA was purified as previously described and then mixed with HeLa extracts supplemented with an ATP regenerating system, ssDNA, and phosphatase inhibitors. The phosphorylated RPA was then purified again as described previously. RAD52 was purified in Ryan Jensen's lab as described previously (6).

DNA binding assay. RPA and pRPA were incubated at indicated concentrations in 35 mM HEPES, NaOH (pH 7.5), 1 mM dithiothreitol (DTT), and 5 nM 80-mer (5′ IRD700-labeled oligonucleotide [TT TGT TAA AAT TCG CGT TAA ATT TTT GTT AAA TCA GCT CAT TTT TTA ACC AAT AGG CCG AAA TCG GCA AAA TCC CTT ATA]; Integrated DNA Technologies [IDT]; high-performance liquid chromatography [HPLC] purified) at 37°C for 5 min. Reactions were then cross-linked for 10 min at room temperature with 0.2% glutaraldehyde and stopped with 100 mM Tris (pH 8.0). Reaction products were loaded on a 1% agarose gel for 2 h and imaged on a Li-Cor Odyssey CLx system.

Substrates for DNA annealing assays. DNA annealing assays were based on experiments reported in reference 6 and performed as follows. Polyacrylamide gel electrophoresis (PAGE)-purified oligonucleotide substrates were obtained from Sigma or IDT. The following oligonucleotides were used: RJ-167-mer (5′-CTGCTTTAT CAAGATAATTTTTCGACTCATCAGAAATATCCGTTTCCTATATTTATTCCTATTATGTTTTATTCATTTACTTATTCTTTATGTT CATTTTTTATATCCTTTACTTTATTTTCTCTGTTTATTCATTTACTTATTTTGTATTATCCTTATCTTATTTA-3′), RJ-Oligo1 (5′-TAATACAAAATAAGTAAATGAATAAACAGAGAAAATAAAG-3′), and RJ-Oligo2 (5′-CTTTATTTTCTCTGTTTATTCATTTA CTTATTTTGTATTA-3′).

DNA annealing assays. Cold 167-mer at 4 nM (molecules) and 5′ radiolabeled oligonucleotide 1 at 2 nM (molecules) were each incubated separately in 10-μl reaction mixtures containing 25 mM Tris acetate (pH 7.5), 1 mM $MgCl_2$, and 1 mM DTT for 5 min with RPA (50 nM), pRPA (50 nM), or storage buffer. The 40-mer is

complementary to the 167-mer at the 3′ end. All incubations were at 37°C. The oligonucleotides were then incubated with either RAD52 (100 nM) or protein storage buffer for 5 min. The two reaction mixtures were then mixed and incubated for 1, 5, 15, or 30 min to allow annealing. At the indicated time points, aliquots were removed and added to stop buffer (4 mg/mL proteinase K, 1% SDS and 0.2 μM unlabeled Oligo2 [complementary to Oligo1]) for 15 min. Loading dye was then added to the samples, and they were run on precast 6% polyacrylamide gels in Tris-borate-EDTA (TBE) buffer (Life Technologies) for 2 h at 30 V. The gels were dried onto Whatman paper and exposed to a phosphorimager screen overnight. The screens were scanned on a Fujifilm FLA-7000 phosphorimager, and bands were quantified using Quantity One software. The percentage of annealed product was calculated as the radiolabeled product divided by the total radiolabeled input DNA in each lane.

Protein buffers. The buffer for RPA and pRPA was 30 mM HEPES, NaOH (pH 7.8), 0.5% inositol, 0.5 mM EDTA, 1 mM DTT, 250 mM KCl. The buffer for RAD52 was 50 mM Tris-Cl (pH 7.5), 200 mM KCl, 15% glycerol, 10 mM β-mercaptoethanol. The buffer for RAD51 was 20 mM HEPES, NaOH (pH 7.5), 150 mM NaCl, 0.1 mM EDTA, 10% glycerol, 2 mM β-mercaptoethanol.

Statistical analysis. Statistical analysis for the various experiments was performed using GraphPad Prism 9.1.0 software. A P value of <0.05 by the unpaired t test (two tailed) was considered statistically significant.

Data availability. The data that support the findings of this study are presented in the article and are available upon request.

ACKNOWLEDGMENTS

We thank James A. Borowiec for the RPA-WT and RPA-A expression plasmids, Melody Di Bona for helping develop the analysis pipeline for quantifying the immunofluorescence images, Ryan Jensen and Carol Kolar for technical assistance, and Qingwen Zhou and William Holloman for their helpful discussions during the course of the experiments. Last, we thank the members of the Powell lab for helpful discussions. Figures were created with the aid of BioRender.

This work was supported by the National Institutes of Health (CA169306 to S.N.P.).

We declare no conflict of interest. We declare that we have no known competing financial interests or personal relationships that could have appeared to influence the work reported in this paper.

REFERENCES

1. Ciccia A, Elledge SJ. 2010. The DNA damage response: making it safe to play with knives. Mol Cell 40:179–204. https://doi.org/10.1016/j.molcel.2010.09.019.
2. Dueva R, Iliakis G. 2020. Replication protein A: a multifunctional protein with roles in DNA replication, repair and beyond. NAR Cancer 2:zcaa022. https://doi.org/10.1093/narcan/zcaa022.
3. Hartlerode AJ, Scully R. 2009. Mechanisms of double-strand break repair in somatic mammalian cells. Biochem J 423:157–168. https://doi.org/10.1042/BJ20090942.
4. Heyer WD, Ehmsen KT, Liu J. 2010. Regulation of homologous recombination in eukaryotes. Annu Rev Genet 44:113–139. https://doi.org/10.1146/annurev-genet-051710-150955.
5. Shiotani B, Zou L. 2009. Single-stranded DNA orchestrates an ATM-to-ATR switch at DNA breaks. Mol Cell 33:547–558. https://doi.org/10.1016/j.molcel.2009.01.024.
6. Jensen RB, Carreira A, Kowalczykowski SC. 2010. Purified human BRCA2 stimulates RAD51-mediated recombination. Nature 467:678–683. https://doi.org/10.1038/nature09399.
7. Liu J, Doty T, Gibson B, Heyer WD. 2010. Human BRCA2 protein promotes RAD51 filament formation on RPA-covered single-stranded DNA. Nat Struct Mol Biol 17:1260–1262. https://doi.org/10.1038/nsmb.1904.
8. Sung P. 1997. Function of yeast Rad52 protein as a mediator between replication protein A and the Rad51 recombinase. J Biol Chem 272:28194–28197. https://doi.org/10.1074/jbc.272.45.28194.
9. New JH, Sugiyama T, Zaitseva E, Kowalczykowski SC. 1998. Rad52 protein stimulates DNA strand exchange by Rad51 and replication protein A. Nature 391:407–410. https://doi.org/10.1038/34950.
10. Rijkers T, Van Den Ouweland J, Morolli B, Rolink AG, Baarends WM, Van Sloun PP, Lohman PH, Pastink A. 1998. Targeted inactivation of mouse RAD52 reduces homologous recombination but not resistance to ionizing radiation. Mol Cell Biol 18:6423–6429. https://doi.org/10.1128/MCB.18.11.6423.
11. Yamaguchi-Iwai Y, Sonoda E, Buerstedde JM, Bezzubova O, Morrison C, Takata M, Shinohara A, Takeda S. 1998. Homologous recombination, but not DNA repair, is reduced in vertebrate cells deficient in RAD52. Mol Cell Biol 18:6430–6435. https://doi.org/10.1128/MCB.18.11.6430.
12. Liu J, Heyer WD. 2011. Who's who in human recombination: BRCA2 and RAD52. Proc Natl Acad Sci U S A 108:441–442. https://doi.org/10.1073/pnas.1016614108.
13. Feng Z, Scott SP, Bussen W, Sharma GG, Guo G, Pandita TK, Powell SN. 2011. Rad52 inactivation is synthetically lethal with BRCA2 deficiency. Proc Natl Acad Sci U S A 108:686–691. https://doi.org/10.1073/pnas.1010959107.
14. Brouwer I, Zhang H, Candelli A, Normanno D, Peterman EJG, Wuite GJL, Modesti M. 2017. Human RAD52 captures and holds DNA strands, increases DNA flexibility, and prevents melting of duplex DNA: implications for DNA recombination. Cell Rep 18:2845–2853. https://doi.org/10.1016/j.celrep.2017.02.068.
15. Shen Z, Cloud KG, Chen DJ, Park MS. 1996. Specific interactions between the human RAD51 and RAD52 proteins. J Biol Chem 271:148–152. https://doi.org/10.1074/jbc.271.1.148.
16. Hanamshet K, Mazina OM, Mazin AV. 2016. Reappearance from obscurity: mammalian Rad52 in homologous recombination. Genes (Basel) 7:63. https://doi.org/10.3390/genes7090063.
17. Chen R, Wold MS. 2014. Replication protein A: single-stranded DNA's first responder. Bioessays 36:1156–1161. https://doi.org/10.1002/bies.201400107.
18. Xu X, Vaithiyalingam S, Glick Gloria G, Mordes Daniel A, Chazin Walter J, Cortez D. 2008. The basic cleft of RPA70N binds multiple checkpoint proteins, including RAD9, to regulate ATR signaling. Mol Cell Biol 28:7345–7353. https://doi.org/10.1128/MCB.01079-08.
19. Brill SJ, Stillman B. 1991. Replication factor-A from Saccharomyces cerevisiae is encoded by three essential genes coordinately expressed at S phase. Genes Dev 5:1589–1600. https://doi.org/10.1101/gad.5.9.1589.
20. Wang Y, Putnam CD, Kane MF, Zhang W, Edelmann L, Russell R, Carrión DV, Chin L, Kucherlapati R, Kolodner RD, Edelmann W. 2005. Mutation in Rpa1 results in defective DNA double-strand break repair, chromosomal instability and cancer in mice. Nat Genet 37:750–755. https://doi.org/10.1038/ng1587.
21. Hass CS, Gakhar L, Wold MS. 2010. Functional characterization of a cancer causing mutation in human replication protein A. Mol Cancer Res 8:1017–1026. https://doi.org/10.1158/1541-7786.MCR-10-0161.

22. Park MS, Ludwig DL, Stigger E, Lee SH. 1996. Physical interaction between human RAD52 and RPA is required for homologous recombination in mammalian cells. J Biol Chem 271:18996–19000. https://doi.org/10.1074/jbc.271.31.18996.
23. Wang H, Guan J, Wang H, Perrault AR, Wang Y, Iliakis G. 2001. Replication protein A2 phosphorylation after DNA damage by the coordinated action of ataxia telangiectasia-mutated and DNA-dependent protein kinase. Cancer Res 61:8554–8563.
24. Block WD, Yu Y, Lees-Miller SP. 2004. Phosphatidyl inositol 3-kinase-like serine/threonine protein kinases (PIKKs) are required for DNA damage-induced phosphorylation of the 32 kDa subunit of replication protein A at threonine 21. Nucleic Acids Res 32:997–1005. https://doi.org/10.1093/nar/gkh265.
25. Oakley GG, Loberg LI, Yao J, Risinger MA, Yunker RL, Zernik-Kobak M, Khanna KK, Lavin MF, Carty MP, Dixon K. 2001. UV-induced hyperphosphorylation of replication protein a depends on DNA replication and expression of ATM protein. Mol Biol Cell 12:1199–1213. https://doi.org/10.1091/mbc.12.5.1199.
26. Byrne BM, Oakley GG. 2019. Replication protein A, the laxative that keeps DNA regular: the importance of RPA phosphorylation in maintaining genome stability. Semin Cell Dev Biol 86:112–120. https://doi.org/10.1016/j.semcdb.2018.04.005.
27. Shi W, Feng Z, Zhang J, Gonzalez-Suarez I, Vanderwaal RP, Wu X, Powell SN, Roti Roti JL, Gonzalo S, Zhang J. 2010. The role of RPA2 phosphorylation in homologous recombination in response to replication arrest. Carcinogenesis 31:994–1002. https://doi.org/10.1093/carcin/bgq035.
28. Vassin VM, Wold MS, Borowiec JA. 2004. Replication protein A (RPA) phosphorylation prevents RPA association with replication centers. Mol Cell Biol 24:1930–1943. https://doi.org/10.1128/MCB.24.5.1930-1943.2004.
29. Feng J, Wakeman T, Yong S, Wu X, Kornbluth S, Wang XF. 2009. Protein phosphatase 2A-dependent dephosphorylation of replication protein A is required for the repair of DNA breaks induced by replication stress. Mol Cell Biol 29:5696–5709. https://doi.org/10.1128/MCB.00191-09.
30. Lee DH, Pan Y, Kanner S, Sung P, Borowiec JA, Chowdhury D. 2010. A PP4 phosphatase complex dephosphorylates RPA2 to facilitate DNA repair via homologous recombination. Nat Struct Mol Biol 17:365–372. https://doi.org/10.1038/nsmb.1769.
31. Deng X, Prakash A, Dhar K, Baia GS, Kolar C, Oakley GG, Borgstahl GE. 2009. Human replication protein A-Rad52-single-stranded DNA complex: stoichiometry and evidence for strand transfer regulation by phosphorylation. Biochemistry 48:6633–6643. https://doi.org/10.1021/bi900564k.
32. Pierce AJ, Johnson RD, Thompson LH, Jasin M. 1999. XRCC3 promotes homology-directed repair of DNA damage in mammalian cells. Genes Dev 13:2633–2638. https://doi.org/10.1101/gad.13.20.2633.
33. Oakley GG, Tillison K, Opiyo SA, Glanzer JG, Horn JM, Patrick SM. 2009. Physical interaction between replication protein A (RPA) and MRN: involvement of RPA2 phosphorylation and the N-terminus of RPA1. Biochemistry 48:7473–7481. https://doi.org/10.1021/bi900694p.
34. Olson E, Nievera CJ, Klimovich V, Fanning E, Wu X. 2006. RPA2 is a direct downstream target for ATR to regulate the S-phase checkpoint. J Biol Chem 281:39517–39533. https://doi.org/10.1074/jbc.M605121200.
35. Serrano MA, Li Z, Dangeti M, Musich PR, Patrick S, Roginskaya M, Cartwright B, Zou Y. 2013. DNA-PK, ATM and ATR collaboratively regulate p53-RPA interaction to facilitate homologous recombination DNA repair. Oncogene 32:2452–2462. https://doi.org/10.1038/onc.2012.257.
36. Wu X, Yang Z, Liu Y, Zou Y. 2005. Preferential localization of hyperphosphorylated replication protein A to double-strand break repair and checkpoint complexes upon DNA damage. Biochem J 391:473–480. https://doi.org/10.1042/BJ20050379.
37. Stark JM, Pierce AJ, Oh J, Pastink A, Jasin M. 2004. Genetic steps of mammalian homologous repair with distinct mutagenic consequences. Mol Cell Biol 24:9305–9316. https://doi.org/10.1128/MCB.24.21.9305-9316.2004.
38. Lok BH, Carley AC, Tchang B, Powell SN. 2013. RAD52 inactivation is synthetically lethal with deficiencies in BRCA1 and PALB2 in addition to BRCA2 through RAD51-mediated homologous recombination. Oncogene 32:3552–3558. https://doi.org/10.1038/onc.2012.391.
39. Fujimori A, Tachiiri S, Sonoda E, Thompson LH, Dhar PK, Hiraoka M, Takeda S, Zhang Y, Reth M, Takata M. 2001. Rad52 partially substitutes for the Rad51 paralog XRCC3 in maintaining chromosomal integrity in vertebrate cells. EMBO J 20:5513–5520. https://doi.org/10.1093/emboj/20.19.5513.
40. Jensen RB, Ozes A, Kim T, Estep A, Kowalczykowski SC. 2013. BRCA2 is epistatic to the RAD51 paralogs in response to DNA damage. DNA Repair (Amst) 12:306–311. https://doi.org/10.1016/j.dnarep.2012.12.007.
41. Chun J, Buechelmaier ES, Powell SN. 2013. Rad51 paralog complexes BCDX2 and CX3 act at different stages in the BRCA1-BRCA2-dependent homologous recombination pathway. Mol Cell Biol 33:387–395. https://doi.org/10.1128/MCB.00465-12.
42. Whelan DR, Lee WTC, Yin Y, Ofri DM, Bermudez-Hernandez K, Keegan S, Fenyo D, Rothenberg E. 2018. Spatiotemporal dynamics of homologous recombination repair at single collapsed replication forks. Nat Commun 9:3882. https://doi.org/10.1038/s41467-018-06435-3.
43. Hatchi E, Goehring L, Landini S, Skourti-Stathaki K, DeConti DK, Abderazzaq FO, Banerjee P, Demers TM, Wang YE, Quackenbush J, Livingston DM. 2021. BRCA1 and RNAi factors promote repair mediated by small RNAs and PALB2–RAD52. Nature 591:665–670. https://doi.org/10.1038/s41586-020-03150-2.
44. Anantha RW, Vassin VM, Borowiec JA. 2007. Sequential and synergistic modification of human RPA stimulates chromosomal DNA repair. J Biol Chem 282:35910–35923. https://doi.org/10.1074/jbc.M704645200.
45. Liu S, Opiyo SO, Manthey K, Glanzer JG, Ashley AK, Amerin C, Troksa K, Shrivastav M, Nickoloff JA, Oakley GG. 2012. Distinct roles for DNA-PK, ATM and ATR in RPA phosphorylation and checkpoint activation in response to replication stress. Nucleic Acids Res 40:10780–10794. https://doi.org/10.1093/nar/gks849.
46. Liaw H, Lee D, Myung K. 2011. DNA-PK-dependent RPA2 hyperphosphorylation facilitates DNA repair and suppresses sister chromatid exchange. PLoS One 6:e21424. https://doi.org/10.1371/journal.pone.0021424.
47. Soniat MM, Myler LR, Kuo HC, Paull TT, Finkelstein IJ. 2019. RPA phosphorylation inhibits DNA resection. Mol Cell 75:145–153.E145. https://doi.org/10.1016/j.molcel.2019.05.005.
48. Robison JG, Elliott J, Dixon K, Oakley GG. 2004. Replication protein A and the Mre11.Rad50.Nbs1 complex co-localize and interact at sites of stalled replication forks. J Biol Chem 279:34802–34810. https://doi.org/10.1074/jbc.M404750200.
49. Bochkareva E, Kaustov L, Ayed A, Yi G-S, Lu Y, Pineda-Lucena A, Liao JCC, Okorokov AL, Milner J, Arrowsmith CH, Bochkarev A. 2005. Single-stranded DNA mimicry in the p53 transactivation domain interaction with replication protein A. Proc Natl Acad Sci U S A 102:15412–15417. https://doi.org/10.1073/pnas.0504614102.
50. Murphy AK, Fitzgerald M, Ro T, Kim JH, Rabinowitsch AI, Chowdhury D, Schildkraut CL, Borowiec JA. 2014. Phosphorylated RPA recruits PALB2 to stalled DNA replication forks to facilitate fork recovery. J Cell Biol 206:493–507. https://doi.org/10.1083/jcb.201404111.
51. Grimme JM, Honda M, Wright R, Okuno Y, Rothenberg E, Mazin AV, Ha T, Spies M. 2010. Human Rad52 binds and wraps single-stranded DNA and mediates annealing via two hRad52-ssDNA complexes. Nucleic Acids Res 38:2917–2930. https://doi.org/10.1093/nar/gkp1249.
52. Ma CJ, Kwon Y, Sung P, Greene EC. 2017. Human RAD52 interactions with replication protein A and the RAD51 presynaptic complex. J Biol Chem 292:11702–11713. https://doi.org/10.1074/jbc.M117.794545.
53. Stefanovie B, Hengel SR, Mlcouskova J, Prochazkova J, Spirek M, Nikulenkov F, Nemecek D, Koch BG, Bain FE, Yu L, Spies M, Krejci L. 2020. DSS1 interacts with and stimulates RAD52 to promote the repair of DSBs. Nucleic Acids Res 48:694–708. https://doi.org/10.1093/nar/gkz1052.
54. Jackson D, Dhar K, Wahl JK, Wold MS, Borgstahl GE. 2002. Analysis of the human replication protein A:Rad52 complex: evidence for crosstalk between RPA32, RPA70, Rad52 and DNA. J Mol Biol 321:133–148. https://doi.org/10.1016/S0022-2836(02)00541-7.
55. Hays SL, Firmenich AA, Massey P, Banerjee R, Berg P. 1998. Studies of the interaction between Rad52 protein and the yeast single-stranded DNA binding protein RPA. Mol Cell Biol 18:4400–4406. https://doi.org/10.1128/MCB.18.7.4400.
56. Borgstahl GEO, Brader K, Mosel A, Liu S, Kremmer E, Goettsch KA, Kolar C, Nasheuer H-P, Oakley GG. 2014. Interplay of DNA damage and cell cycle signaling at the level of human replication protein A. DNA Repair (Amst) 21:12–23. https://doi.org/10.1016/j.dnarep.2014.05.005.
57. Park MS. 1995. Expression of human RAD52 confers resistance to ionizing radiation in mammalian cells. J Biol Chem 270:15467–15470. https://doi.org/10.1074/jbc.270.26.15467.
58. Liu Y, Maizels N. 2000. Coordinated response of mammalian Rad51 and Rad52 to DNA damage. EMBO Rep 1:85–90. https://doi.org/10.1093/embo-reports/kvd002.
59. Yanez RJ, Porter AC. 2002. Differential effects of Rad52p overexpression on gene targeting and extrachromosomal homologous recombination in a human cell line. Nucleic Acids Res 30:740–748. https://doi.org/10.1093/nar/30.3.740.
60. Kurumizaka H, Aihara H, Kagawa W, Shibata T, Yokoyama S. 1999. Human Rad51 amino acid residues required for Rad52 binding. J Mol Biol 291:537–548. https://doi.org/10.1006/jmbi.1999.2950.

61. Wray J, Liu J, Nickoloff JA, Shen Z. 2008. Distinct RAD51 associations with RAD52 and BCCIP in response to DNA damage and replication stress. Cancer Res 68:2699–2707. https://doi.org/10.1158/0008-5472.CAN-07-6505.
62. Essers J, Houtsmuller AB, van Veelen L, Paulusma C, Nigg AL, Pastink A, Vermeulen W, Hoeijmakers JH, Kanaar R. 2002. Nuclear dynamics of RAD52 group homologous recombination proteins in response to DNA damage. EMBO J 21:2030–2037. https://doi.org/10.1093/emboj/21.8.2030.
63. Davis AP, Symington LS. 2003. The Rad52-Rad59 complex interacts with Rad51 and replication protein A. DNA Repair (Amst) 2:1127–1134. https://doi.org/10.1016/S1568-7864(03)00121-6.
64. Mer G, Bochkarev A, Gupta R, Bochkareva E, Frappier L, Ingles CJ, Edwards AM, Chazin WJ. 2000. Structural basis for the recognition of DNA repair proteins UNG2, XPA, and RAD52 by replication factor RPA. Cell 103:449–456. https://doi.org/10.1016/S0092-8674(00)00136-7.
65. Singleton MR, Wentzell LM, Liu Y, West SC, Wigley DB. 2002. Structure of the single-strand annealing domain of human RAD52 protein. Proc Natl Acad Sci U S A 99:13492–13497. https://doi.org/10.1073/pnas.212449899.
66. Reddy G, Golub EI, Radding CM. 1997. Human Rad52 protein promotes single-strand DNA annealing followed by branch migration. Mutat Res 377:53–59. https://doi.org/10.1016/S0027-5107(97)00057-2.
67. Van Dyck E, Stasiak AZ, Stasiak A, West SC. 2001. Visualization of recombination intermediates produced by RAD52-mediated single-strand annealing. EMBO Rep 2:905–909. https://doi.org/10.1093/embo-reports/kve201.
68. Rothenberg E, Grimme JM, Spies M, Ha T. 2008. Human Rad52-mediated homology search and annealing occurs by continuous interactions between overlapping nucleoprotein complexes. Proc Natl Acad Sci U S A 105:20274–20279. https://doi.org/10.1073/pnas.0810317106.
69. Rueden CT, Schindelin J, Hiner MC, DeZonia BE, Walter AE, Arena ET, Eliceiri KW. 2017. ImageJ2: ImageJ for the next generation of scientific image data. BMC Bioinformatics 18:529. https://doi.org/10.1186/s12859-017-1934-z.
70. Bolte S, Cordelières FP. 2006. A guided tour into subcellular colocalization analysis in light microscopy. J Microsc 224:213–232. https://doi.org/10.1111/j.1365-2818.2006.01706.x.
71. Nuss JE, Patrick SM, Oakley GG, Alter GM, Robison JG, Dixon K, Turchi JJ. 2005. DNA damage induced hyperphosphorylation of replication protein A. 1. Identification of novel sites of phosphorylation in response to DNA damage. Biochemistry 44:8428–8437. https://doi.org/10.1021/bi0480584.